Transient Effect in Fluorescence Quenching by Electron Transfer. 4. Long-Range Electron Transfer in a Nonpolar Solvent

Laure Burel,[†] Mehran Mostafavi,[‡] Shigeo Murata,* and M. Tachiya

National Institute of Materials and Chemical Research, 1-1 Higashi, Tsukuba, Ibaraki 305-8565, Japan

Received: March 30, 1999; In Final Form: May 18, 1999

The transient effect in fluorescence quenching observed in a viscous nonpolar solvent, liquid paraffin, was measured and analyzed in order to study the mechanism of electron transfer fluorescence quenching in such solvents. The method of analysis is similar to that adopted in previous papers (*J. Phys. Chem.* **1995**, *99*, 5354; **1996**, *100*, 4064) to study electron transfer in polar solvents. The difference from the previous method is that a function of the form $A \exp[-b(r - r_0)]$ was used as the electron transfer rate constant $k(r)$ instead of the Marcus equation and that the dependence of the steady-state fluorescence intensity on the quencher concentration was also analyzed in addition to the fluorescence decay at high quencher concentrations ($\geq$50 mM). The parameters A and b and the diffusion coefficient D were determined from these analyses. The distribution of quenching distance was calculated using these parameter values. The distribution shows that the quenching occurs at distances longer than the contact distances of the fluorescer and quencher molecules. It was concluded that, even in nonpolar liquid paraffin, quenching occurs by long-range electron transfer rather than by exciplex formation as long as the ΔG of electron transfer is negative and far from 0 eV. The relation between electron transfer and exciplex formation in nonpolar solvents was discussed.

1. Introduction

Fluorescence quenching is very often used to study photoinduced electron transfer reactions. In solution, the quenching process consists of two steps: diffusion of fluorescer and quencher molecules and electron transfer. The latter step is sometimes very fast compared to the former, and the whole quenching process is diffusion controlled. In this case, the quenching rate constant obtained experimentally contains little information about electron transfer. On the other hand, if the quencher concentration is high enough, the "transient effect" is observed; that is, fluorescence decay becomes nonexponential at short times. In the short-time region, the quenching rate is affected by the electron transfer step as well as by the diffusional step. Consequently, the electron transfer step can be studied by analyzing the transient effect in an appropriate manner. Studies along this line have been done for more than 20 years.[1−13]

In previous papers,[9−13] we conducted experiments in polar solvents and analyzed the result using the Collins−Kimball model of diffusion-controlled reactions[9] or the diffusion equation combined with the Marcus equation of electron transfer.[10−13] In refs 10−12, we determined experimentally the distance dependence of the electron transfer rate constant and obtained the distribution of electron transfer distance using this dependence.

Fluorescence is also quenched by electron transfer in nonpolar solvents. It has been established that the mechanism of quenching changes with solvent polarity.[14,15] In polar solvents, fluorescence is quenched by full electron transfer from the donor to the acceptor and the resulting ions can be detected by transient absorption spectroscopy. Experimental results concerning electron transfer in polar solvents have been discussed using the Marcus theory. In nonpolar solvents, on the other hand, the ions cannot be detected. Instead, a new emission due to an exciplex formed by the donor and the acceptor is often observed. In the exciplex state, the donor and the acceptor are in contact. These results led people to believe that the quenching in nonpolar solvents occurs via exciplex formation, which implies that the donor and the acceptor are in contact when quenching occurs.

In the present paper, we report the distance dependence of the rate constant of fluorescence quenching determined experimentally in a nonpolar solvent, liquid paraffin. The results show that even in the nonpolar solvent long-range electron transfer can take place between the donor and the acceptor.

2. Experimental Section

The solvent to be used in this study should be highly viscous in order for two quenching parameters A and b (see the next section) to be determined simultaneously from experiment. This has been shown in a previous paper.[10] Liquid paraffin is the only nonpolar solvent we found which satisfies this condition. Liquid paraffin purchased from Merck (spectroscopic grade, Uvasol) was passed through an alumina column. After this treatment, the absorbance at 275 nm was less than 0.15. The viscosity of this solvent was determined using a glass viscometer to be 104 cP at 296 K.

9-Cyanoanthracene (CA) and 9,10-dicyanoanthracene (DCA) were used as fluorescers (electron acceptors, A), and *N*,*N*,*N*′,*N*′-tetramethyl-*p*-phenylenediamine (TMPD), *N*,*N*-dimethylaniline (DMA), and *p*-dimethoxybenzene (DMB) served as quenchers (electron donors, D). CA, DCA, and DMB were recrystallized several times from appropriate solvents. TMPD was precipitated from its dihydrochloride and was sublimed in a vacuum. DMA was distilled under reduced pressure. There are not many electron donors soluble in liquid paraffin to high concentrations

[†] Address from September 1999 on: UMR6521, Département de Chimie, Université Brest, 6 av. Le Gorgeu, 29285 Brest cedex, France.

[‡] Permanent address: Laboratoire de Physico-Chimie des Rayonnements, UMR 8610, CNRS/Université Paris-Sud, Centre d'Orsay, Bât 350, 91405 ORSAY, France.

10.1021/jp991087h CCC: $18.00
Published on Web 07/14/1999

(>0.1 M), and we could not find many D−A pairs suitable for this study. Upon addition of quenchers, the absorption of the fluorescers becomes slightly weaker and a weak absorption due to a ground-state complex is detected on the longer wavelength side. However, even at the highest quencher concentration (0.2 M), the change in the absorption intensity was ∼5%. Because the change was small, it was not taken into account in the analysis of the steady-state fluorescence intensity ratio described later.

In the fluorescence decay measurement, fluorescence was excited at 400 nm using the second harmonic of a mode-locked Ti:sapphire laser output (pulse duration ≈ 100 fs), and the decay curves were measured by time-correlated single-photon counting. The apparatus has been described elsewhere.[9,10] The fwhm of the instrument response function was ∼60 ps.

Measurements of fluorescence decay curves and stationary fluorescence intensities were made at 296 K. They were detected at 440 and at 470 nm. In this study, it is necessary to detect just the fluorescence of the acceptor and not that of the exciplex. At higher quencher concentrations (0.15−0.2 M), very weak exciplex fluorescence can be detected with a maximum at 650 nm (in the case of the DCA−DMA pair, uncorrected for spectral response of the apparatus), at 580 nm (DCA−DMB), and at 710 nm (DCA−TMPD). Since the exciplex fluorescence is very weak and its spectrum is far away from the observation wavelengths, the influence of the exciplex fluorescence on the observed fluorescence decay and intensity is considered negligible. Indeed, the decay curves and stationary intensities observed at 440 and 470 nm were the same within experimental error.

3. Data Analysis

The method of data analysis employed in this paper is similar to those described in previous papers[10−13] for fluorescence quenching in a polar solvent. It is described here briefly. For simplicity, it is assumed that A is excited and its fluorescence quenched by D. The fluorescence decay curve $P(t)$ in the presence of quencher is given by[10]

$$P(t) = \exp[-t/\tau_0 - 4\pi c_0 \int_d^\infty \{1 - U(r,t)\} r^2 \, dr] \qquad (1)$$

where τ_0, c_0, and d are the fluorescence lifetime in the absence of quencher, the quencher concentration, and the sum of the molecular radii of D and A, respectively. $U(r,t)$ is the survival probability of a D−A* pair at time t which was separated by distance r when A was excited at $t = 0$. $U(r,t)$ satisfies the following differential equation:[10]

$$\frac{\partial U(r,t)}{\partial t} = D\left[\frac{\partial^2}{\partial r^2} + \frac{2}{r}\frac{\partial}{\partial r}\right] U(r,t) - k(r)U(r,t) \qquad (2)$$

where D is the sum of the diffusion coefficients of the donor and the acceptor and $k(r)$ is the first-order quenching rate constant. In previous papers, the Marcus equation of electron transfer was used for $k(r)$, since in polar solvents quenching is considered to be due to full electron transfer. In nonpolar solvents, quenching may be caused by exciplex formation or by full electron transfer. Although the distance dependence of the rate constant of exciplex formation is not known, as the first approximation it may be approximated as an exponential function. The distance dependence of the Marcus equation is also approximated as an exponential function.[10,11] We thus assume the following equation for $k(r)$:

$$k(r) = A \exp[-b(r - r_0)] \qquad (3)$$

A and b are the parameters characterizing the rate and are to be determined experimentally. $A = k(r_0)$ and $r_0 = 6$ Å in this paper.

Equation 2 coupled with eq 3 must be solved under appropriate initial and boundary conditions. This was solved numerically using the Crank−Nicholson method. Both the temporal and spatial regions were divided into ∼1000 steps. Since $U(r,t)$ changes more rapidly at shorter times, smaller temporal step sizes were employed at shorter times. At very short times (<1 ps), this treatment was not enough and oscillations were sometimes observed in calculated $U(r,t)$. At such short times, $U(r,t) = \exp(-k(r)t)$ was used instead of the numerical solution of eq 2. This can be justified since the diffusion coefficient D in liquid paraffin is small and diffusion of the donor and the acceptor at such short times can be neglected.

We see from eqs 1−3 that the shape of the decay curve is determined by the three parameters A, b, and D. Therefore, in principle, it is possible to determine these parameter values by fitting the calculated decay curve $P(t)$ (eq 1) to the measured ones (actually, in the fitting not $P(t)$ itself but the convolution of $P(t)$ with the instrument response function is used as the calculated decay curve). In practice, however, it has been shown in a previous paper[10] that it is impossible to determine more than two parameters simultaneously and that, to determine the two parameters simultaneously, the experiment should be done in a solvent of high viscosity. Thus, we selected liquid paraffin as a solvent in the present work, as described above. The diffusion coefficient D of the molecules was estimated from the Stokes−Einstein equation

$$D = kT/x\pi\eta r_a \qquad (4)$$

where η and r_a are the viscosity of the solvent and the radius of the diffusing molecule, respectively.[16] r_a was estimated following Edward[17] and Bondi.[18] The values of r_a thus estimated are (in angstroms) CA, 3.6; DCA, 3.7; TMPD, 3.5; DMB, 3.2; and DMA, 3.2. The magnitude of x will be discussed in the next section. The fitting of the calculated decay curve to the measured ones was made by a nonlinear least-squares method based on the Marquardt algorithm.

Experimental decay curve data were accumulated until the channel corresponding to the maximum acquired 10 000 counts. The fitting was made from a channel of about 5000 counts in the rise-up region (this channel is hereafter referred to as the first fit channel). The time shift between the measured decay curve and the instrument response function was adjusted so that the convoluted curve best reproduces the rise-up region of the measured decay curve.

Integration of the fluorescence decay curve $P(t)$ gives the steady-state intensity I. So the intensity ratio I_0/I is given by the following equation:

$$I_0/I = \frac{\tau_0}{\int_0^\infty P(t)\, dt} \qquad (5)$$

where I_0 and I are steady-state fluorescence intensities in the absence and in the presence of quencher, respectively. The distribution of quenching distance $Y(r)$ is given by the following equation:[11,12,19,20]

$$Y(r) = 4\pi r^2 c_0 k(r) \int_0^\infty q(r,t)\, P(t)\, dt \qquad (6)$$

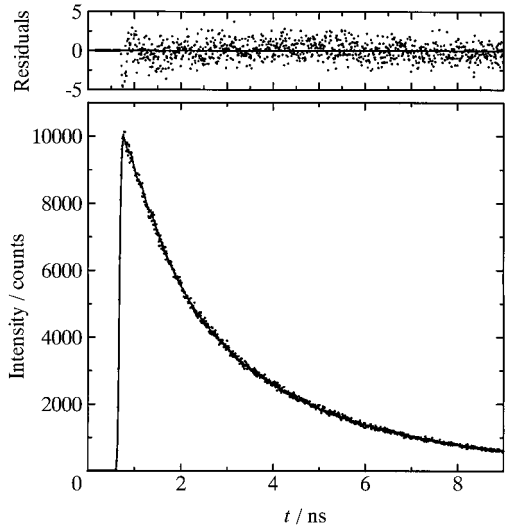

Figure 1. Observed (dots) and calculated best-fit (solid line) decay curves of DCA fluorescence quenched by TMPD (0.15 M) in liquid paraffin at 296 K. The calculation of the decay curve was made using eqs 1−4 with $x = 1.6$ in eq 4, and its convolution with the observed instrument response function was fitted to the observed decay curve by a least-squares method. The best-fit parameters determined from this calculation are $A = 3.7 \times 10^{14}$ s^{-1} and $b = 1.3$ Å^{-1}.

TABLE 1: Parameter Values Obtained by Fitting Eq 1 to the Observed Decay Curve of DCA Fluorescence Quenched by 0.15 M TMPD in Liquid Paraffin[a]

x	D (10^{-5} cm^2 s^{-1})	A (s^{-1})	b (Å^{-1})	χ^2
1.0	0.070	9.7×10^{10}	0.70	1.5330
1.2	0.058	2.6×10^{11}	0.76	1.2393
1.4	0.050	1.2×10^{13}	1.1	1.2554
1.6	0.044	3.7×10^{14}	1.3	1.2728
1.8	0.039	1.1×10^{16}	1.5	1.2891
2.0	0.035	3.2×10^{17}	1.7	1.3064
2.2	0.032	9.7×10^{18}	1.9	1.3251
2.5	0.028	1.9×10^{21}	2.2	1.3544
2.7	0.026	7.8×10^{22}	2.4	1.3745
2.9	0.024	2.7×10^{24}	2.6	1.3940

[a] In the fitting, D values corresponding to the x values given here are assumed and A and b were determined by a least-squares method.

where $q(r,t) = c(r,t)/c_0$, with $c(r,t)$ being the concentration profile of the quencher. $q(r,t)$ satisfies eq 2 with $U(r,t)$ replaced by $q(r,t)$. Consequently, $Y(r)$ can be calculated if the rate parameters A and b and the diffusion coefficient D are known. In this work, A, b, and D have been determined by analyzing the experimental results. All the calculations including the integrals in eqs 5 and 6 were carried out numerically.

4. Results

4.1. Determination of the Parameters *A*, *b*, and *D* from the Fluorescence Decay Curve and the Steady-State Intensity. Figure 1 shows the observed fluorescence decay curve (dots) of the DCA−TMPD (0.15 M) pair and the best-fit calculated curve (solid line) corresponding to $D = 0.0436 \times 10^{-5}$ cm^2 s^{-1} ($x = 1.6$ in eq 4). From this fitting, A and b were determined to be 7.5×10^{13} s^{-1} and 1.3 Å^{-1}, respectively. In the same way, A and b corresponding to several x values have been determined and are shown in Table 1 together with the weighted residuals χ^2 of the fitting. Table 1 shows that the fitting is almost equally good for D values corresponding to x values lying between 1.2 and 2. This implies that it is almost impossible to determine A, b, and D simultaneously by the fitting, as described in the previous section.

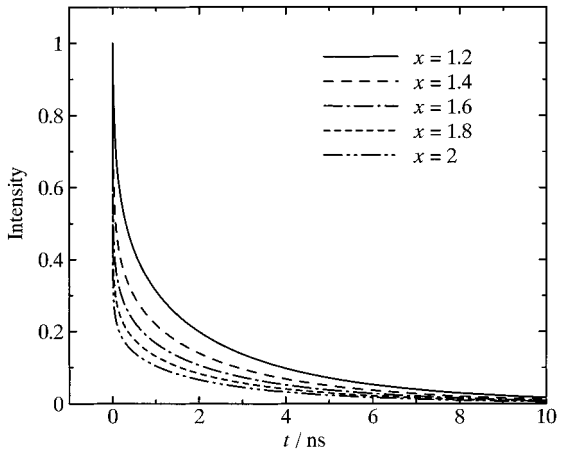

Figure 2. Fluorescence decay curves calculated using eqs 1−4 for DCA−TMPD (0.15 M). The values of A and b obtained for different x values shown in Table 1 were used.

In a previous paper,[10] $x = 5$ was assumed in eq 4 to obtain the diffusion coefficients in ethylene glycol. In the present study, $x = 5$ did not give good fits. As described above, the fitting becomes better for x values between 1.2 and 2. These x values are very different from $x = 6$, appropriate for large solute molecules diffusing in a solvent consisting of small molecules, and from $x = 4$, appropriate for solute and solvent molecules of similar sizes.

Amu[21] reported the diffusion coefficient of cyclohexylbromide in various paraffin hydrocarbons. He found that in these solvents x is not a constant but decreases with increasing chain length of the hydrocarbons; that is, x corresponding to *n*-heptadecane (C_{17}) is about 1.8 times smaller than that corresponding to *n*-hexane (C_6). Similar results concerning the diffusion coefficient in paraffin hydrocarbons have been reported very recently by Kowert et al.[22] Since liquid paraffin consists of paraffin hydrocarbons much larger than C_{17}, our finding that x values lie between 1.2 and 2 is consistent with their results. The weighted residuals χ^2 seems to have the minimum value near $x = 1.2$. However, as stated above, the fits with x lying between 1.2 and 2 give almost equally good results and it is difficult to determine the value of x from these fittings. Thus, we need additional data to determine x (or D).

Table 1 shows that, although the fitting is reasonably good for x values between 1.2 and 2, the magnitude of A and b strongly depends on x; larger x yields larger A and b. Figure 2 shows the fluorescence decay curves calculated with eq 1 using A and b shown in Table 1 (corresponding to x between 1.2 and 2). The curves have been normalized to unity at $t = 0$. It is apparent from Figure 2 that the decay curves corresponding to different x values are considerably different. Nevertheless, the convoluted decay curves are all very similar. The reason for this is that the instrument response function has a fwhm of ∼60 ps. The initial fast decay seen in Figure 2 is not observed in the convoluted curves.

The steady-state fluorescence intensity, on the other hand, is given by the area under the decay curve itself and has nothing to do with the response function of the decay curve measurement system. Consequently, the difference between the decay curves corresponding to different x values seen in Figure 2 is directly reflected in the steady-state intensity. Figure 3 shows the experimental and calculated intensity ratios I_0/I for the DCA−TMPD pair as functions of TMPD concentration. Calculated intensity ratios were obtained using eq 5 with A and b corresponding to several x values. As seen in Figure 3, the

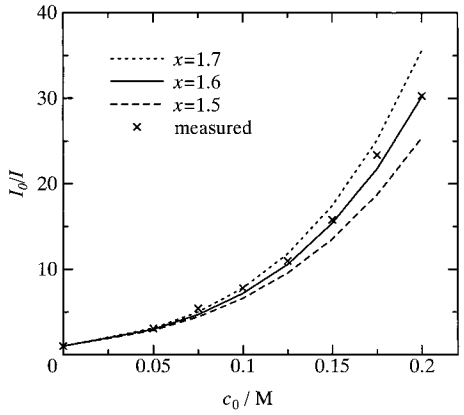

Figure 3. Fluorescence intensity ratio for DCA−TMPD pair as a function of quencher concentration. The solid and broken lines indicate the results of calculations using eq 5 with *D* obtained from eq 4.

TABLE 2: Parameters *A*, *b*, and *D* Determined by Analyzing the Fluorescence Decay Curve and the Steady State Fluorescence Intensity Ratio[a]

acceptor	donor (concn (M))	ΔG^{AN} (eV)	*A* (s^{-1})	*b* ($Å^{-1}$)	*D* ($\times 10^{-5}$ cm^2 s^{-1})
DCA	TMPD (0.15)	−1.87	3.7×10^{14}	1.3	0.0436
DCA	TMPD (0.20)	−1.87	8.2×10^{13}	1.2	0.0436
CA	TMPD (0.15)	−1.46	3.2×10^{15}	1.6	0.0444
CA	TMPD (0.20)	−1.46	1.7×10^{15}	1.5	0.0444
DCA	DMA (0.15)	−1.21	3.4×10^{16}	1.9	0.0459
DCA	DMA (0.20)	−1.21	2.9×10^{17}	2.1	0.0459
CA	DMA (0.15)	−0.73	3.2×10^{17}	3.7	0.0467
DCA	DMB (0.15)	−0.67	9.7×10^{20}	4.3	0.0457

[a] ΔG^{AN} is the free energy change associated with electron transfer in acetonitrile. $x = 1.6$ was used for all the D−A pairs for the reason described in the text.

calculated intensity ratios are rather sensitive to the change in *x* as long as *A* and *b* values obtained by fitting the decay curve are used. It is apparent that $x = 1.6$ gives the best fit to the experimental intensity ratios. From this value, $D = 0.0436 \times 10^{-5}$ cm^2 s^{-1} was obtained for the DCA−TMPD pair. *A* and *b* corresponding to this value of *D* are 3.7×10^{14} s^{-1} and 1.3 $Å^{-1}$, respectively.

Our procedure of determining *A*, *b*, and *D* values is summarized as follows. First, several *D* values are assumed, and *A* and *b* are determined by fitting the calculated decay curve to the measured one. Several sets of *A*, *b*, and *D* values thus obtained are used to calculate the fluorescence intensity ratios at high quencher concentrations and the set which best reproduces the ratios is selected. In principle, an alternative method is possible in which the intensity ratios are first used to determine *A* and *b* by the least-squares method. This method, however, does not yield good results, since the number of points of the intensity ratio data is not enough (typically <10) and the least-squares method does not work well.

4.2. Distance Dependence of the Quenching Rate Constant and Distribution of Quenching Distance. By the method described in the previous section, we have determined *A*, *b*, and *D* for several D−A pairs with different ΔG^{AN} values in a nonpolar solvent, liquid paraffin. The results are summarized in Table 2. ΔG^{AN} is the free energy change associated with electron transfer in acetonitrile. It was determined using the redox potentials of D and A, together with the excitation energy of A. Of course, ΔG of the quenching reaction in liquid paraffin is different from ΔG^{AN}. Here ΔG^{AN} is used simply as a measure of the driving force of the quenching reaction. In general, the fitting of the decay curve was more successful for D−A pairs with larger $-\Delta G^{AN}$ values. The fitting was tried over various fitting ranges by changing the last fit channel (with the first fit channel fixed, as described in the data analysis section). The values of *A*, *b*, and *D* for the DCA−TMPD pair remained practically unchanged over various fitting ranges. This was also true for CA−TMPD and DCA−DMA pairs. On the other hand, the values for DCA−DMB and CA−DMA depended on the fitting range, and sometimes the fitting yielded unrealistic results. The values given in Table 2 for these two pairs are, therefore, considered not very accurate.

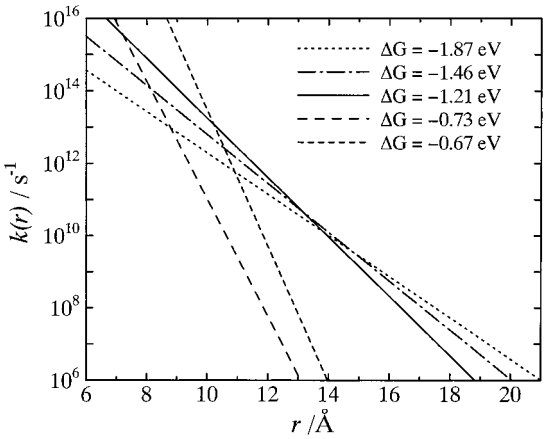

Figure 4. First-order quenching rate constant as a function of distance. The parameters *A* and *b* determined experimentally at a quencher concentration of 0.15 M are used. The ΔG values correspond to the D−A pairs given in Table 2.

The fitting to the fluorescence intensity ratio yielded *x* values lying between 1.5 and 1.7 for the five pairs investigated in the present work. Since these values are considered to be constant within experimental error, we hereafter employ $x = 1.6$ for all the pairs. Table 2 gives the values corresponding to $x = 1.6$. *A* and *b* values obtained for the same D−A pairs at different donor concentrations (0.15 and 0.2 M) agree reasonably well.

The quenching rate constant calculated from *A* and *b* is plotted against D−A distance in Figure 4. It is seen from Figure 4 that the slope changes with ΔG^{AN}; it increases with the decrease in $-\Delta G^{AN}$. This change of the slope is also found at 0.2 M as seen in Table 2. This is in contrast to the result in a polar solvent, ethylene glycol, reported in a previous paper.[10] In this solvent, the slope is practically unchanged with the change in ΔG^{AN}.

In addition to this, the rate constant in liquid paraffin is larger than that in ethylene glycol. In ref 10, $x = 5$ was assumed to obtain the diffusion coefficient. In that work, the steady-state fluorescence intensity ratio was not measured to determine *x* experimentally, because a certain amount of ground-state complex was found and it prevented accurate determination of the fluorescence intensity ratio. However, even if this uncertainty in *D* is taken into consideration, the first-order rate constant in liquid paraffin still seems larger than that in ethylene glycol.

Figure 5 shows the distribution of quenching distance calculated from eq 6 using *A*, *b*, and *D* given in Table 2. Each curve has a maximum at a longer distance and a plateau in the short-distance region. The existence of the maximum can be understood in the same way as in the case of electron transfer in a polar solvent.[11] It can be explained briefly as follows. The electron transfer rate is large enough at the distance corresponding to the maximum in $Y(r)$ and a large fraction of D−A* pairs is lost there, with only a small fraction left for further approach. Consequently, at shorter distances, electron transfer becomes less efficient despite the increase of the rate constant. The plateau is mostly due to those D−A* pairs which were already

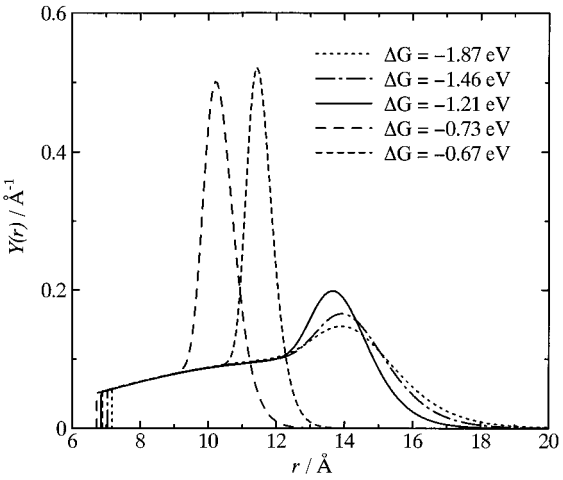

Figure 5. Distribution of quenching distance at a quencher concentration of 0.15 M. ΔG is the free energy change associated with electron transfer in acetonitrile.

present in this region when excitation was made. At short distances, the curves overlap with each other almost completely. This is because electron transfer in this region is fast and occurs before the diffusion of D and A*, which is slow since the solvent viscosity is high. The sharp maximum found in the distribution for pairs with smaller $-\Delta G^{AN}$ values is due to the sharp increase of the rate constant at the corresponding distance.

It is seen from Figure 5 that the quenching can occur at distances longer than the contact distances. The quenching distance seems to be distributed up to even longer distances than in the case of electron transfer in a polar solvent.[11] This is mainly because the rate constant is larger in liquid paraffin. Another reason is that the diffusion coefficient in liquid paraffin is about half of that in ethylene glycol. As has been shown,[11] a smaller diffusion coefficient causes the distribution of quenching distance to shift toward longer distances.

5. Discussion

As has been described in the Introduction, fluorescence quenching in nonpolar solvents is often accompanied by exciplex emission. The formation of the exciplex is represented by the following scheme:

$$A^* + D \rightleftarrows (A^{\delta-}D^{\delta+})^* \qquad (7)$$

The right-hand side of eq 7 represents the exciplex. In general, the backward reaction to give the excited state of the acceptor should be taken into account. In that case, eq 2 and thus the whole analysis will be much more complicated. In the present case, however, the backward reaction does not seem important. There are some reasons why we assume this.

(1) ΔG^{AN} of forward electron transfer measured in acetonitrile may be used as a measure of driving force of the quenching reaction. Therefore, the rate of backward reaction is more or less correlated with ΔG^{AN} in a series of D−A pairs; that is, if $-\Delta G^{AN}$ is larger, the rate of backward reaction is considered to be lower. The backward reaction has been shown to occur in D−A pairs in a nonpolar solvent with $-\Delta G^{AN}$ not far from 0 eV. For example,[23] the pyrene-*N*,*N*-dimethylaniline system in which exciplex fluorescence has been extensively studied has a ΔG^{AN} value of ∼−0.4 eV. The D−A pairs employed in this study have ΔG^{AN} values of electron transfer ranging from −1.87 to −0.67 eV.

(2) The fluorescence of the exciplex formed by the D−A pairs studied in this work is extremely weak. This probably implies that the exciplex fluorescence lifetime is short. This makes the backward reaction less probable.

(3) If the backward reaction is important at room temperature, fluorescence will be less quenched at higher temperatures. This is because the backward reaction has higher activation energy compared to the forward reaction. In our measurement, fluorescence quenching was more efficient at higher temperatures for all the pairs studied in this work.

Unfortunately, these are indirect evidences and may not be enough to exclude the possibility of the backward reaction. However, since the decay curves of DCA−TMPD, CA−TMPD, and DCA−DMA pairs are very well reproduced by eq 1 by adjusting the parameters, we believe that the backward reaction can be neglected and the parameter values obtained for these three pairs are more reliable. On the other hand, for DCA−DMB and CA−DMA pairs, which have smaller $-\Delta G^{AN}$ values, the transient effect was smaller and the curves were less reproducible. The parameter values obtained from the analysis are thus considered not very accurate. Nevertheless, the results are considered accurate at least qualitatively, since we always observed similar trends in different experiments for DCA−DMB and CA−DMA pairs.

The distribution of quenching distance given in Figure 5 shows that the quenching mainly occurs at distances longer than the contact distances. At such long distances, the interaction between D and A is not strong enough to form the exciplex. The quenching is considered to occur by long-range electron transfer rather than by exciplex formation. This is evidence showing that fluorescence is quenched by long-range electron transfer not only in polar solvent but also in nonpolar solvent. For pairs with smaller $-\Delta G^{AN}$, long-range electron transfer will be less probable, since its rate decreases with decreasing $-\Delta G^{AN}$ as predicted by the Marcus theory. It is interesting to see that for two pairs with smaller $-\Delta G^{AN}$ values quenching occurs at shorter distances than for the other three.

As seen from Figure 4, the slope of the $k(r)$ vs r plot increases with the decrease in $-\Delta G^{AN}$. The distance dependence of electron transfer rate constant in nonpolar solvent can be described by the Marcus equation corrected for the contribution of intramolecular vibration,[24,25]

$$k(r) = \frac{2\pi}{\hbar} J_0^{\,2} \exp[-\beta(r - r_0)] \frac{1}{\sqrt{4\pi\lambda_S k_B T}} \sum_{m=0}^{\infty} \frac{e^{-S} S^m}{m!} \exp\left[-\frac{(\Delta G + \lambda_S + m h\nu)^2}{4\lambda_S k_B T}\right] \qquad (8)$$

where J_0 is the transfer integral at distance r_0, β its attenuation coefficient with distance, λ_S the solvent reorganization energy, and ν the frequency of the intramolecular vibration. $S = \lambda_i/h\nu$, with λ_i being the vibrational reorganization energy. In nonpolar solvents λ_S is generally small and is estimated to be ∼0.1 eV. Figure 6 shows the plot of eq 8 with $J_0 = 100$ cm^{-1} at 6 Å, $\beta = 1$ Å^{-1}, $\nu = 1500$ cm^{-1}, and $\lambda_i = 0.3$ eV. The free energy change ΔG^{LP} of electron transfer in liquid paraffin was obtained from ΔG^{AN} using the following equation:

$$\Delta G^{LP} = \Delta G^{AN} + \frac{e^2}{2}\left(\frac{1}{\epsilon_s} - \frac{1}{\epsilon_s^{AN}}\right)\left(\frac{1}{r_D} + \frac{1}{r_A} - \frac{2}{r}\right) \qquad (9)$$

The second term on the right-hand side accounts for the

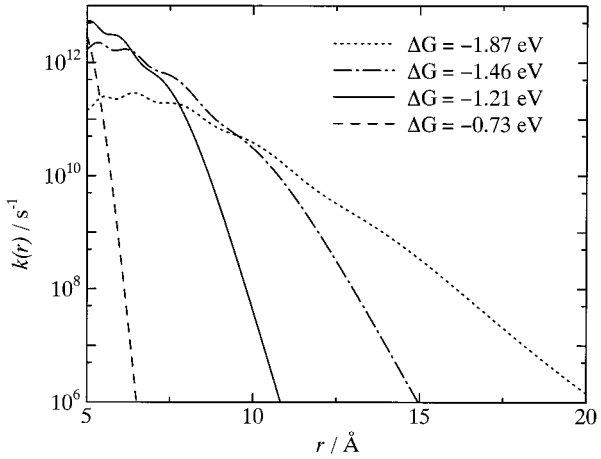

Figure 6. Calculated first-order electron transfer rate constant. Equation 7 was used for the calculation. See the text for parameter values adopted.

difference between the free energy change of solvation in acetonitrile and that in liquid paraffin. The maxima and shoulders seen in each curve in Figure 6 correspond to the contributions from different m's in eq 8. It is apparent from Figure 6 that the slope increases with the decrease in $-\Delta G^{AN}$. This result is in qualitative agreement with Figure 4 obtained experimentally and is consistent with the above conclusion that long-range electron transfer is responsible for the fluorescence quenching.

It is necessary to discuss the magnitude of the parameters A and b in eq 3. Comparison of eqs 3 and 8 shows that eq 3 has a large number of parameters combined into the constants A and b. b is proportional to the slope of the $k(r)$ vs r plot, but is different from β in eq 8. A is proportional to J_0^2, but its magnitude strongly depends on ΔG. This is seen in Figure 6 (in which $J_0 = 100$ cm^{-1} was assumed for all the D−A pairs) by extrapolating the long-distance part of each curve to $r = 6$ Å. The result of analysis in Table 2 showing very different A values for different D−A pairs is, therefore, not unreasonable.

According to eq 9, ΔG^{LP} remains positive at $r > 5$ Å for a D−A pair with $\Delta G^{AN} = -0.67$ eV. This implies that full electron transfer is not probable for this pair and suggests the exciplex mechanism for fluorescence quenching. In the exciplex state, D and A are in contact and strong interaction between them makes ΔG of the reaction (the free energy change between the D + A* and the exciplex states) more negative than that expected for long-range electron transfer. It is considered that the mechanism of fluorescence quenching in nonpolar solvent changes according to the value of ΔG^{AN}: if the D−A pair has larger $-\Delta G^{AN}$, fluorescence is quenched by full (long range) electron transfer, while for a pair with smaller $-\Delta G^{AN}$, exciplex formation is responsible for quenching.

In polar solvents, the ion pairs resulting from long-range electron transfer can dissociate to form free ions. The dissociation will be less probable in nonpolar solvents, since the Coulombic interaction between the ions is less shielded. If the ions approach each other to the contact distance in nonpolar solvent, it may lead to the formation of exciplex as well as to the deactivation to the ground state.

A conclusion similar to the above one has been drawn for D−A pairs which are connected by semiflexible groups. Verhoeven et al.[26−28] studied these systems extensively. They connected the D and A components by the semiflexible groups to reduce the rate of approach of the two components. In a nonpolar solvent, they were able to detect charge transfer emission from the extended CT state which was formed by long-range electron transfer. They also detected the emission from the exciplex state which was formed from the extended CT state after the D^+ and A^- components have approached each other by Coulombic interaction.

6. Concluding Remarks

In this paper, we have determined experimentally the parameters of fluorescence quenching rate constant in nonpolar solvent together with the diffusion coefficient. Using these parameters, we have shown that the mechanism of fluorescence quenching in the nonpolar solvent changes depending on ΔG of the reaction. The mechanism changes from long-range electron transfer to exciplex formation when $-\Delta G^{AN}$ is decreased. This change in the mechanism is very similar to that in a polar solvent, acetonitrile, reported by Kikuchi et al.[29,30] According to them, the quenching mechanism in acetonitrile changes from long-range electron transfer to exciplex formation when $-\Delta G^{AN}$ is decreased and the change occurs at $\Delta G^{AN} = -0.5$ eV.

The electron transfer rate constant in liquid paraffin is larger than that in ethylene glycol. The origin of this difference is not clear yet. The size of the solvent molecule may have something to do with this. If the solvent molecule separating D and A* is larger, the D−A* interaction has more through-bond character. This will lead to a larger transfer integral and therefore to a larger electron transfer rate.

Acknowledgment. The authors are grateful to Dr. Kazuhiko Seki for fruitful discussion concerning the use of the Stokes−Einstein equation.

References and Notes

(1) See for recent review: Sikorski, M.; Krystkowiak, E.; Steer, R. P. *J. Photochem. Photobiol. A: Chem.* **1998**, *117*, 1.
(2) Angel, S. A.; Peters, K. S. *J. Phys. Chem.* **1989**, *93*, 713.
(3) Angel, S. A.; Peters, K. S. *J. Phys. Chem.* **1991**, *95*, 3606.
(4) Eads, D. D.; Dismer, B. G.; Fleming, G. R. *J. Chem. Phys.* **1990**, *93*, 1136.
(5) Scully, A. D.; Hirayama, S.; Fukushima, K.; Tominaga, T. *J. Phys. Chem.* **1993**, *97*, 10524.
(6) Nishikawa, T.; Asahi, T.; Okada, T.; Mataga, N.; Kakitani, T. *Chem. Phys. Lett.* **1991**, *185*, 237.
(7) Song, L.; Dorfman, R. C.; Swallen, S. F.; Fayer, M. D. *J. Phys. Chem.* **1991**, *95*, 3454.
(8) Swallen, S. F.; Weidemaier, K.; Tavernier, H. L.; Fayer, M. D. *J. Phys. Chem.* **1996**, *100*, 8106.
(9) Murata, S.; Nishimura, M.; Matsuzaki, S. Y.; Tachiya, M. *Chem. Phys. Lett.* **1994**, *219*, 200.
(10) Murata, S.; Matsuzaki, S. Y.; Tachiya, M. *J. Phys. Chem.* **1995**, *99*, 5354.
(11) Murata, S.; Tachiya, M. *J. Phys. Chem.* **1996**, *100*, 4064.
(12) Murata, S.; Tachiya, M. *J. Chim. Phys.* **1996**, *93*, 1577.
(13) Iwai, S.; Murata, S.; Tachiya, M. *J. Chem. Phys.* **1998**, *109*, 5963.
(14) See, for example: Birks, J. B. *Photophysics of Aromatic Molecules*; John Wiley & Sons: New York, 1970.
(15) Mataga, N. *Pure Appl. Chem.* **1984**, *56*, 1255.
(16) The viscosity of the solution changes by the addition of quencher. For instance, the viscosity of liquid paraffin containing 0.15 M TMPD is 87.5 cP at 296 K. The value 104 cP of the pure solvent was nevertheless used as η to calculate D by eq 4, since the volume fraction of the added TMPD is small (of the order of 1%) compared to that of the solvent and the molecules are considered to diffuse in an environment which is approximately the same as that of the pure solvent. The change in the η value affects the A and b values obtained by the procedure described later, but does not affect the qualitative conclusion of this paper.
(17) Edward, J. T. *J. Chem. Educ.* **1970**, *47*, 261.
(18) Bondi, A. *J. Phys. Chem.* **1964**, *64*, 441.

(19) Burshtein, A. I. *Chem. Phys. Lett.* **1992**, *194*, 247.
(20) Burshtein, A. I.; Krissinel, E.; Mikhekasvili, M. S. *J. Phys. Chem.* **1994**, *98*, 7319.
(21) Amu, T. C. *J. Chem. Soc., Faraday Trans. 1* **1979**, *75*, 1226.
(22) Kowert, B. A.; Dang, N. C. *J. Phys. Chem. A* **1999**, *103*, 779.
(23) Okada, T.; Matsui, H.; Oohari, H.; Matsuo, H.; Mataga, N. *J. Chem. Phys.* **1968**, *49*, 4717.
(24) Ulstrup, J.; Jortner, J. *J. Chem. Phys.* **1975**, *63*, 4358.
(25) Miller, J. R.; Beitz, J. V.; Huddleston, R. K. *J. Am. Chem. Soc.* **1984**, *106*, 5057.
(26) Verhoeven, J. W.; Scherer, T.; Willemse, R. J. *Pure Appl. Chem.* **1993**, *65*, 1717.
(27) Wegewijs, B.; Ng, A. K. F.; Verhoeven, J. W. *Recl. Trav. Chim. Pays-Bas* **1995**, *114*, 6.
(28) Jäger, W.; Schneider, S.; Verhoeven, J. W. *Chem. Phys. Lett.* 1997, *270*, 50.
(29) Kikuchi, K.; Niwa, T.; Takahashi, Y.; Ikeda, H.; Miyashi, T.; Hoshi, M. *Chem. Phys. Lett.* **1990**, *173*, 421.
(30) Niwa, T.; Kikuchi, K.; Matsusita, N.; Hayashi, M.; Katagiri, T.; Takahashi, Y.; Miyashi, T. *J. Phys. Chem.* **1993**, *97*, 11960.